

# We are IntechOpen, the world's leading publisher of Open Access books Built by scientists, for scientists

6,900

Open access books available

185,000

International authors and editors

200M

Downloads

Our authors are among the

154

Countries delivered to

TOP 1%

most cited scientists

12.2%

Contributors from top 500 universities



WEB OF SCIENCE™

Selection of our books indexed in the Book Citation Index  
in Web of Science™ Core Collection (BKCI)

Interested in publishing with us?  
Contact [book.department@intechopen.com](mailto:book.department@intechopen.com)

Numbers displayed above are based on latest data collected.  
For more information visit [www.intechopen.com](http://www.intechopen.com)



# Animal Pain Models for Spinal Cord Stimulation

*Joseph M. Williams, Courtney A. Kelley, Ricardo Vallejo,  
David C. Platt and David L. Cedeño*

## Abstract

Spinal cord stimulation (SCS) is an electrical neuromodulation technique with proven effectiveness and safety for the treatment of intractable chronic pain in humans. Despite its widespread use, the mechanism of action is not fully understood. Animal models of chronic pain, particularly rodent-based, have been adapted to study the effect of SCS on pain-like behavior, as well as on the electrophysiology and molecular biology of neural tissues. This chapter reviews animal pain models for SCS, emphasizing on findings relevant to advancing our understanding of the mechanism of action of SCS, and highlighting the contribution of the animal model to advance clinical outcomes. The models described include those in which SCS has been coupled to neuropathic pain models in rats and sheep based on peripheral nerve injuries, including the chronic constriction injury (CCI) model and the spared nerve injury model (SNI). Other neuropathic pain models described are the spinal nerve ligation (SNL) for neuropathic pain of segmental origin, as well as the chemotherapy-induced and diabetes-induced peripheral neuropathy models. We also describe the use of SCS with inflammatory pain and ischemic pain models.

**Keywords:** spinal cord stimulation, animal models, neuropathic pain, inflammatory pain, ischemia

## 1. Introduction

The field of electrical neuromodulation was developed under the hypothesis that the activation of large, myelinated nerve fibers could modulate sensory nociceptive signals carried by A-delta and C nerve fibers into the dorsal horn in the spinal cord. The gate control theory (GCT) formulated by Melzack and Wall [1], served as inspiration for the use of peripheral nerve stimulation and spinal cord stimulation (SCS) to treat pain. The simplicity of the proposed mechanism, based on the understanding of pain in 1965, granted researchers with the ability to formulate finite mathematical and complex computational models to assess the effects of different variables of the electrical signal on the neuronal conduction. The GCT's enduring value in neuromodulation for more than 50 years is due to its simplicity and utility as a working tool to postulate therapies to patients in pain. Unfortunately, as the German psychologist Wolfgang Köhler explains: "premature simplifications and systematization in science, could ossify science and prevent vital growth" [2].

The early 1990s marked the beginning of a revolution in the field of neuroscience in understanding the mechanism of pathological pain from a molecular perspective. The use of animal models has helped unravel the role of neuroinflammatory

processes driven by glial cells in the development and maintenance of chronic neuropathic pain. Those advances though, were largely neglected in the field of electrical neuromodulation, which remained focused on the effects of electrical signals on neuronal conduction, ignoring the benefit of understanding how these signals could affect biological processes at the neuron-glia interaction. The differential electrophysiological characteristics of neurons and glial cells is now at the core of our quest to understand how electrical signals affect such biological processes. To begin with, the resting membrane potential of these cell populations is different, driven by the fact that the main neuronal intracellular cation is potassium, while sodium is the predominant one in glial cells [3]. Considering the critical roles that various specialized glial cell populations play in the intimate communication between neurons and glial cells, it is pertinent to briefly describe these roles. Following peripheral injury, persistent release of neurotransmitters at the synaptic cleft activates microglial and astrocyte membrane receptors generating transcriptional changes that generate the synthesis and release of pro-inflammatory and anti-inflammatory cytokines. Astrocytes are critical to maintain homeostasis at the synapse. The synaptic cleft is surrounded by astroglial perisynaptic processes in what is now known as the tripartite synapse. Perisynaptic glial processes are densely packed with numerous transporters, which provide proper homeostasis of ions and neurotransmitters in the synaptic cleft, for local metabolism support, and for release of astroglia-derived scavengers of oxygen species [4]. For example, membrane ionotropic and metabotropic glutamate receptors in the astrocyte regulate glutamate concentration. Interestingly, a single astrocyte provides processes that extend over distance to surround over 100,000 synapses. During intense neuronal firing, the release of neurotransmitters, such as glutamate and GABA, induces the elevation of calcium ion concentrations in glial cells, causing  $\text{Ca}^{2+}$ -dependent release of molecules that affects neural excitability and synaptic transmission and plasticity. Even more thought-provoking is that although astrocytes are unable to generate action potentials, they can raise intracellular calcium concentrations that spread from astrocyte to astrocyte through gap channels that allow propagation of so-called calcium waves as a way of cell-to-cell communication. The presence of  $\text{Ca}^{2+}$  mobilizations mediated by astrocytes implies that glial cells have some excitability and neuromodulator activities [5]. Finally, oligodendrocytes provide myelin to hundreds of surrounding axons and are known to affect the conduction velocity of action potentials propagating along the axons they surround when electrically stimulated [6].

An important distinction between glial cells and neurons is that glial cells depolarize following electrical stimulation, but do not generate action potentials. In 1981, Roitbak and Fanardjian [7] demonstrated in a live feline model that changes in the frequency and intensity of the applied pulsed electrical signals could lead to differential degrees of astrocytic depolarization. Another interesting clue on how electrical signals could affect glial cells was provided by Agnesi et al. [8], in an experiment with anesthetized rats that showed that changing the repolarization of an electrical stimulation signal from monophasic to a biphasic led to different degrees of glutamate release by the stimulated astrocytes.

The complexity of changes in neuron-glia biological processes triggered by pain and further modulation by electrical stimulation demands the use of experimental animal models. Testing such hypotheses in humans would require large-scale, well-controlled clinical trials because of the heterogeneity of genetics and pain etiology in the general population [9].

The notable anatomical, biological, and physiological resemblances between humans and animals, predominantly mammals, have encouraged researchers to investigate a large range of mechanisms and assess novel therapies in animal models before applying their discoveries to humans.

Scientists cross-examine organisms at multiple levels: molecules, cells, organs, and physiological functions in healthy or diseased conditions. Advance molecular technologies are required to get a complete portrayal and understanding of the mechanisms. Certain aspects of the responses can be evaluated using in vitro approaches (e.g., cell culture). On the other hand, the exploration of physiological functions and systemic interactions between organs requires a whole organism.

This chapter explores the efforts of diverse research groups to understand from a behavioral and molecular perspective, how spinal cord stimulation affects pathological pain by utilizing animal models. This research may provide strong hypotheses on what may be happening in humans and ways to continue improving therapeutic efficacy.

The following sections provide a description of existing, well-validated models for pain caused by neuropathies, inflammation, and ischemic conditions. Due to technical limitations, most of these are based on *Rattus norvegicus*, although recently models in a larger animal (*Ovis aries*) have been developed.

## **2. Animal models of SCS for neuropathic pain**

Neuropathic pain is caused by damaged somatosensory neural circuits that have developed into a disease condition as a result of an injury that compromised nerve fibers. Chronic neuropathic pain affects hundreds of millions of people around the world and is one of the main sources of work-related disabilities, contributing to the socioeconomical burden on individuals as well as health systems [10]. SCS is largely indicated for chronic neuropathic pain conditions, thus the development of various animal models that resemble clinical conditions play a critical role in our understanding of the electrophysiological and molecular changes in the establishment and persistence of neuropathic pain.

### **2.1 SCS in partial nerve injury models**

Prior to the development of the chronic constriction injury (CCI) model, animal models of pain often were lacking in their ability to accurately mimic human peripheral neuropathological conditions or did not reflect conditions involving injuries which spared a portion of a nerve's functioning [11]. The CCI model most commonly used was described by Bennet and Xie in 1988 [11]. The procedure typically involves exposing the common sciatic nerve under anesthesia at the level of the mid-thigh and freeing approximately 7 mm of the sciatic nerve from adhering tissue at a location proximal to the sciatic nerve's trifurcation. Once exposed, four sutures are tied loosely around the sciatic nerve approximately 1-2 mm apart from one another. These ligatures are tied loose enough to just barely constrict the diameter of the sciatic nerve (as observed under 25x-40x magnification), thus preserving partial nerve functioning [11-16]. Constriction of the sciatic nerve was observed histologically beneath all 4 ligature areas as early as one day following the CCI procedure. From days 2-21, adjacent constriction areas tended to progressively merge and were accompanied by thinning of the affected sciatic nerve area. Two to four months after the CCI procedure, thinning of the ligated area was still present, but the swellings typically observed in the area had dissipated.

Importantly, this CCI model has proven to be effective in eliciting a neuropathic pain state as measured by a variety of methods, including von Frey mechanical, chemogenic, and heat and cold thermal stimulation. CCI surgery typically resulted in increased paw sensitivity following von Frey stimulation by Day 2 post-lesion using both the up-down method of analysis [12, 15, 16] and the ascending filament

method of analysis [12–14]. The CCI model is also sensitive to chemogenic pain. Following the application of a noxious substance (a 50% mustard oil solution) to the affected hind paw, CCI rats exhibited exaggerated physical responses and an increase in the amount of time they held their hind paw above the floor of the apparatus [11]. CCI rats also showed hypersensitivity to noxious heat sources, such as radiant beams of light being applied to the affected hind paw [11, 16] and increased allodynic responses to cold, such as a slightly chilled metal floor [11].

Although most applications of the CCI model with SCS have been performed in rats, an ovine model has also been effectively demonstrated [17]. In rats, application of SCS with pulsed signals at 50 Hz frequency, 0.2 ms pulse width (PW), and intensity at 66% of the motor threshold (MT) for 30 minutes [12, 14] decreased pain sensitivity following CCI, but did not return pain levels back to pre-injury control levels. Similar results were obtained when SCS was applied for 180 minutes in rats with CCI lesions using the following SCS parameters: 50 Hz frequency, 0.2 ms PW at 80% of the MT [12]. Lowering the intensity to 20–40% of the MT eliminated the beneficial effect of SCS. Electrodes in these rat studies were aimed at the T11-L1 regions of the spinal cord. In sheep, SCS parameters were set at 40 Hz frequency, 120  $\mu$ s PW and 0.1 V intensity on a continuous setting for one week with electrodes placed at the L2-L3 region. SCS also attenuated pain responses following CCI in sheep, though also failed to return pain levels back to pre-lesion levels [17]. Most SCS studies following CCI typically utilized conventional (also called tonic) SCS at a stimulating frequency of 50 Hz. However, a more detailed investigation of frequency on treatment outcomes (in which frequency varied from 1 Hz to 150 Hz) found a response curve that suggested that while the GCT could account for a subset of efficacious SCS responses, it is unlikely to be the only mechanism underlying the beneficial effects of SCS [18].

In addition to demonstrating that SCS was effective in decreasing pain sensitivity, the CCI model also has proven valuable in elucidating the biological mechanisms behind the increase in pain following injury and the beneficial effect of SCS. After CCI lesions, rats exhibited an increase in the toll-like receptor 4 and nuclear factor  $\kappa$ B [15, 16], which subsequently could increase the release of pro-inflammatory cytokines such as IL-1 $\beta$ , IL-6, and TNF- $\alpha$ . SCS significantly reduced these CCI-induced increases, perhaps by inhibiting the activation of glial cells. Indeed, the co-administration of the microglial inhibitor minocycline was shown to decrease CCI-induced pain and prolonged the effect of SCS [12]. However, this same study also showed an increase in the microglial-reactive marker OX-42 and the astrocyte reactive marker GFAP in the lumbar region of CCI-lesioned rats following SCS treatment. This paradoxical increase may limit the effectiveness of SCS and may partially explain why SCS is not effective in all patients and why pain relief often does not return to baseline levels following SCS. Other studies utilizing SCS in CCI-lesioned rats have identified roles of the adenosine and GABAergic systems in mediating the beneficial effects of SCS. Administration of adenosine or the adenosine A1 receptor agonist R-N6-phenylisopropyladenosine (R-PIA), decreased pain in CCI rats [14]. In addition, giving sub-effective doses of R-PIA to non-responders to SCS during stimulation led to effective pain relief. Zhang et al. [18] also found that administration of bicuculline, a GABA<sub>A</sub> receptor antagonist, decreased inhibitory responses to SCS.

Although the CCI model has provided significant value in (1) serving as a valid model of neuropathic pain, (2) demonstrating that the use of SCS is effective in reducing neuropathic pain, and (3) advancing our understanding of the biological mechanisms underlying SCS, its use has perhaps been surpassed in recent years by another animal model of partial nerve injury called partial sciatic nerve ligation (PSNL). Most PSNL studies utilize the Seltzer technique [19]. The procedure typically involves exposing the sciatic nerve under anesthesia at high-thigh level. The sciatic nerve is freed from adhering tissue at a location near the trochanter just distal to the point at

which the posterior biceps semitendinosus nerve branches off the common sciatic nerve. Once the sciatic nerve is properly exposed, a suture with a curved cutting mini needle is inserted into the nerve. Unlike the CCI procedure, which involves a loose ligation of the sciatic nerve, the PSNL procedure involves tightly ligating approximately 1/3 to 1/2 of the dorsal nerve thickness [19, 20]. As with the CCI procedure, the goal is to partially reduce, but not completely block sciatic nerve functioning.

Similar to the CCI model, the PSNL model also successfully induces a neuropathic pain state as measured by a variety of methods. The primary method is to assess mechanical allodynia using von Frey filaments [21–23]. Following PSNL surgery, rats show a decreased paw withdrawal response following mechanical stimulation of the affected paw, as compared to control rats, pre-surgery baseline levels, and paw withdrawal thresholds (PWT) following stimulation of the contralateral, unaffected paw [23, 24]. This increased pain sensitivity usually develops by Day 2 post-PSNL lesion [21] and is still typically observed after two weeks post-PSNL lesion [20, 24, 25]. Meuwissen et al. [26] recorded decreased PWT over 40 days following the PSNL lesion. Although the PSNL technique overall has been successful in inducing a neuropathic pain state, it should be noted that there is a wide range of pain responsiveness across studies, with some studies reporting 100% of subjects exhibiting hyperalgesia with von Frey testing of the affected hind paw [20, 24] and other studies reporting less than 40% of subjects showing hyperalgesia [27, 28]. Increased paw sensitivity to thermal stimuli has also been observed following the presentation of both heat stimuli (e.g., a radiant light beam) and cold stimuli, such as a cold spray directed at the affected paw [19, 29]. However, the degree of thermal sensitivity can vary depending upon the location of the PSNL ligature. Other studies have also confirmed hypersensitivity to pain following PSNL surgery by using a pneumatic pressure device [30] and by observing gait/posture [31]. Overall, the PSNL technique has proven successful at inducing a neuropathic pain state as assessed by numerous methodologies.

The PSNL model has also proven effective at evaluating SCS treatment for chronic neuropathic pain. Both tonic and burst SCS attenuated the pain sensitivity observed in rat PSNL neuropathic pain models [20, 24]. In rats, tonic SCS (50 Hz frequency, 0.2 ms PW, intensity at 66% of the MT) attenuated PSNL-induced hyperalgesia following 30 minutes of stimulation [23, 32, 33] and 60 minutes of stimulation [20, 22, 24]. Though tonic SCS successfully decreased pain sensitivity, SCS treatment typically did not return pain levels in rats back to pre-injury control levels. In a mouse model, SCS treatment following PSNL lesions proved particularly efficacious, with 80% of mice in one study [34] and 100% of mice in another study [25] responding positively to tonic SCS treatment. In this latter study, unlike the typical rat study, the mice returned to baseline levels of paw withdrawal following SCS treatment.

Although most rat studies investigating the effect of SCS following PSNL lesions have utilized conventional stimulation parameters and have shown a significant benefit of tonic SCS treatment, it is clear that not all PSNL rat subjects benefit from SCS treatment, leading researchers to investigate different SCS parameters in hopes of improving efficacy. Some factors that have proved to have significant impact on SCS efficacy following PSNL lesions include: (1) electrode placement, (2) stimulus intensity, (3) timing of treatment, and (4) utilizing a burst (vs tonic) stimulation pattern. Electrodes placed at the T13 level of the spinal cord typically yielded more efficacious treatment outcomes than electrodes placed at the T11 area [28, 31, 35] or L5 and L6 regions [36]. In a study that directly compared the efficacy of electrode location at T13 and T11 [21], the T13 placement yielded significantly better pain relief than placement at T11 with 63% vs 15% improvement, respectively, following 15 minutes of electrical stimulation and 48.5% vs. 18.4% improvement, respectively, following 30 minutes of electrical stimulation. Lowering the intensity to

30-50% of the MT reduced the beneficial effect of tonic SCS [24]. In terms of timing, early SCS treatment given within 24 hours of lesion led to significantly better treatment outcomes than late SCS given 16 days post-lesion [32]. Interestingly, an early round of SCS treatment followed by a subsequent late round of SCS treatment increased the efficacy of the late SCS treatment [37]. Lastly, burst stimulation typically led to similar response rates as tonic stimulation [20, 22, 26]. However, burst stimulation patterns did produce slightly different outcomes. For instance, one study [24] found that tonic SCS was most effective at 66% of the MT, while burst SCS was most effective at 50% of the MT. In addition, burst stimulation took longer following stimulus onset to achieve therapeutic benefits, but the benefits of the burst stimulation lasted longer after the stimulation was turned off [38]. Burst SCS stimulation also led to greater performance than tonic SCS on a mechanical conflict avoidance system (MCAS) task which measured the cognitive-motivational aspects of pain, rather than the more typical mechanical allodynic physical response to pain [26]. These results suggest that although equally efficacious, tonic, and burst SCS stimulation may work, at least in part, by different biological mechanisms.

Given the beneficial effect of SCS treatment following PSNL lesions, many PSNL studies have sought to investigate the biological mechanisms behind it. Many studies have utilized a paradigm in which sub-effective doses of pharmaceutical treatments are given to SCS non-responders to determine if the combination of these treatments can yield beneficial effects. Song et al. [29] showed that sub-effective doses of the muscarinic agonist oxotremorine turned SCS non-responders into SCS responders, suggesting that the cholinergic system (particularly M2 and M4 muscarinic receptors) plays an important role in SCS efficacy. A subsequent study by these same authors [39] indicated an important serotonergic role in the pain-relieving effect of SCS, particularly the 5-HT<sub>2A</sub> and 5-HT<sub>4</sub> serotonin receptor subtypes. Similarly, blocking NMDA receptors with sub-effective doses of ketamine followed by 30 minutes of SCS also turned SCS non-responders into SCS responders, indicating that the glutamate system also plays an important role in the beneficial effects of SCS [22]. While blocking the excitatory glutamatergic system likely plays a role in successful SCS treatment, enhancing the inhibitory GABAergic system might also play a significant role in successful SCS treatment [27, 32]. SCS treatment decreased intracellular GABA levels in SCS responders but not SCS non-responders [32], while increasing extracellular GABA levels in the spinal cord [27]. Lastly, SCS stimulation in PSNL rats also led to an increase in levels of *c-fos*, suggesting immediate early gene modulation may trigger longer term changes which could explain pain relief both during and after SCS stimulation [40]. Overall, PSNL has proven to be a valuable tool in examining the biological mechanisms behind the beneficial treatment effects of SCS.

## 2.2 SCS in the spared nerve injury model

The Spared Nerve Injury (SNI) was developed by Decosterd and Woolf in 2000 [41] to evaluate peripheral neuropathic pain in the rat model. The SNI is considered superior to previous denervation and partial denervation models due to its specificity of the affected region, as well as its prompt and long-lasting effect. Unlike other models that were designed to test acute nociceptive pain through behavioral and electrophysiological measurements, denervation and partial denervation models induce sensations such as hypersensitivity that more accurately reflect true clinical chronic pain conditions.

The SNI procedure targets the sciatic nerve at its point of trifurcation (**Figure 1A**) in the hindlimb of the rat. Located directly under the biceps femoris muscle, the nerves are exposed and identified as the tibial, common peroneal, and

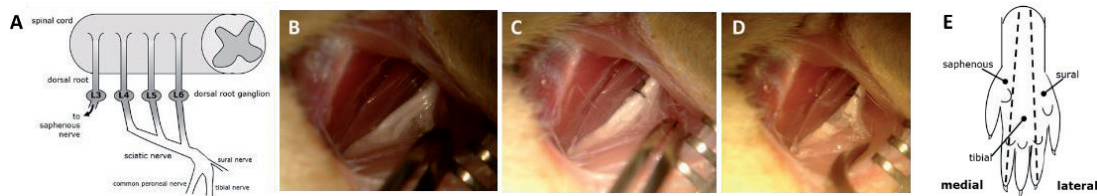


**Figure 1.**

(A) A scheme depicting the anatomical innervation of the sciatic nerve into the spinal cord of the rat. (B-D) Photographic sequence of the localization, ligation, and sectioning of the tibial and peroneal nerves. (E) Map of nerve coverage to plantar hind paw surfaces.

sural branches (**Figure 1B**). Distal to the point of trifurcation and in the direction of the terminal end, both the tibial and common peroneal branches are individually ligated with silk sutures (**Figure 1C**). Then, 2–4 mm of nerve is sectioned and removed to ensure a complete disruption of nerve transmission (**Figure 1D**). The incision is then closed, leaving the sural branch fully intact and undisturbed. Minor amendments, such as carefully separating the gluteus superficialis and biceps femoris muscles instead of cutting through to expose the sciatic nerve, were made in some later studies in attempt to reduce unnecessary tissue damage [42]. Hypersensitivity is rapidly established in this model, with behavioral onset occurring at just 24 hours post-induction, lasting no less than 6 months, with peak sensitivity around 2 weeks [41]. The duration of the SNI effectiveness allows for considerable flexibility when considering study design. Per the original study, non-responders are virtually nonexistent so long as the model is induced correctly.

As shown in **Figure 1E**, the hind paw of the rat is subdivided into three zones which are innervated by the sciatic and saphenous nerves. Transecting two of the three sciatic nerve branches, allows for precise and consistent behavioral testing of the lateral portion of plantar surface, corresponding to the sural nerve. This model permits mechanical and thermal allodynia, as well as thermal hyperalgesia to be evaluated [41] and has been used extensively in basic science studies investigating the use spinal cord stimulation (SCS) for the treatment of neuropathic pain.

In 2015, the SNI-SCS model was taken a step further when Tilley et al. [42] developed a model of continuous stimulation in an awake and freely moving rat, allowing stimulation to be delivered for 72 continuous hours. This method allowed for more clinically relevant testing since human patients receive continuous stimulation. A miniaturized four-electrode cylindrical lead was implanted in the epidural space of the rat and anchored into the musculature in the back (**Figure 2**). The lead exited through the incision and was secured through a custom-made harness and tubing up to a circuit board and stimulator suspended in a swivel so that the full assembly could turn and move with the rat. The rat cage lid was modified to allow free movement of the tubing. In later studies, the lead has been attached to an ethernet port secured to the rat harness with a coiled ethernet cord running to the stimulator connector suspended in the swivel [43]. Mechanical (von Frey filament) and cold thermal (acetone drop) allodynia were tested in this study. SCS was set at 50 Hz frequency, 20  $\mu$ s PW, and at 70% of the MT. While there was no apparent improvement in cold allodynia following SCS, mechanical allodynia was significantly alleviated 24 and 72 hours after the start of SCS. A follow-up genomic study revealed the biological processes uniquely modulated by the SNI model and SCS in the spinal cord and dorsal root ganglion tissues (**Table 1**) [44]. The primary affected processes in both types of tissues included inflammatory response, ion channel regulation, and immune response.

Following the initial development of the SNI model, Li et al. [35] tested variations in an effort to optimize the model specifically for SCS studies. The study included the original SNI procedure, peroneal axotomy, tibial axotomy, tibial tight ligation (no sectioning), and partial tibial ligation (1/3 to 1/2 of its diameter ligated,

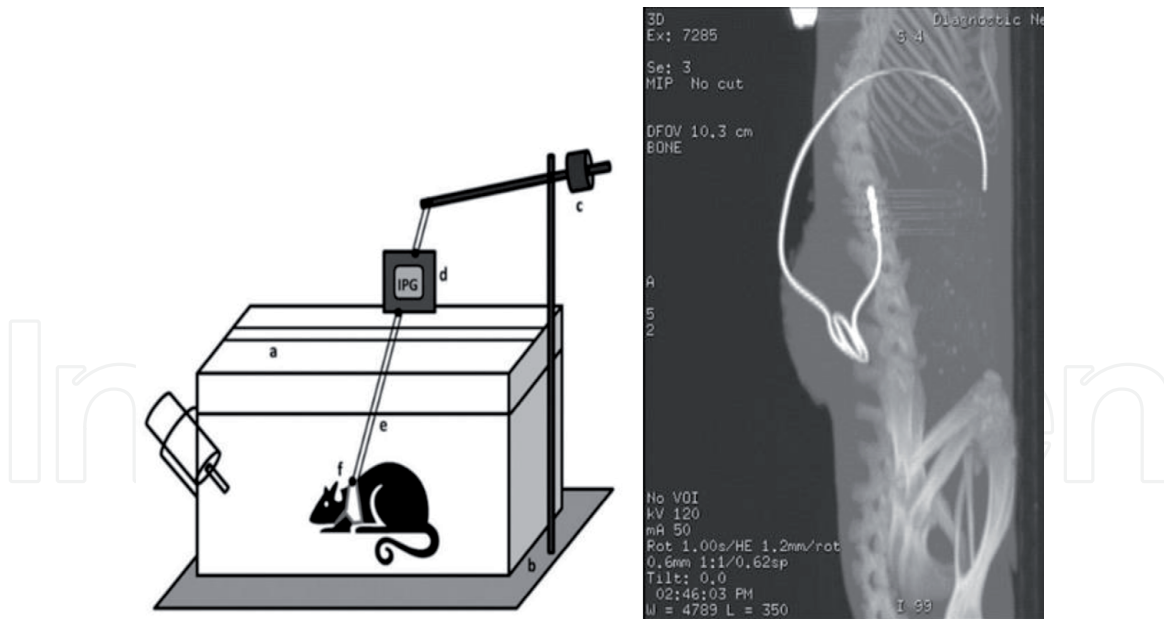


**Figure 2.**

Left: A diagram of the setup for continuous SCS setup reported in references [42, 44]. a: plexiglass lid, b: supporting floor, c: counterweight swivel system, d: connecting board/stimulator (IPG), e: connecting cable, f: harness with lead connector. Right: a lateral x-ray image showing a quadripolar SCS lead placed in the dorsal epidural space of a rat.

without sectioning). SCS was delivered through an implanted 2 mm disc cathode placed on the dura at the T11 level. The 4 mm anode was placed on the chest wall, subcutaneously. Stimulation parameters were set at 50 Hz frequency, 0.2 ms PW, and amplitude at 90% of the MT. SCS was delivered for a 30-minute duration. Measuring mechanical allodynia via von Frey filament testing, authors found that all variations of the model produced allodynia within one week, lasting for at least 3 weeks. All variations except the partial tibial ligation lasted 7-10 weeks. Paw posture was noted as one difference between models, where peroneal axotomy resulted in an inverted position of the paw which tended to be dragged behind the rat. The other variations presented an eversion posture, with the partial tibial ligation being less prominent. Contrary to the original study, where no non-responders were reported and the contralateral hypersensitivity rate was zero, Li et al. found only 53% of SNI operated rats developed hypersensitivity and 25% had some hypersensitivity in the contralateral paw. Response to SCS showed the SNI group with the smallest responder rate at just 8%, compared to the 40-50% responder rate of the variation groups. The researchers concluded there was an inverse relationship between degree of hypersensitivity and efficacy of SCS, agreeing with previous literature in similar models [45], and that these variations of the SNI may provide better models for use in SCS animal studies. However, it should be mentioned that some later studies report higher responder rates to the original variation of the SNI model and subsequent SCS treatment.

Most recently, Sluka and coworkers [46] evaluated tonic SCS on multiple pain models, including the SNI. Implanting an epidural lead and corresponding neurostimulator, the rats were stimulated for 15 minutes per day at 60 Hz, 0.25 ms PW, and at 90% of the MT. Two weeks after SNI induction, the effect of SCS was evaluated. They found that neuropathic pain was alleviated by tonic SCS, measured by von Frey filaments, with significantly increased withdrawal thresholds. Twenty-four hours after stimulation was turned off, behavioral testing revealed that the effect of SCS was lost. The authors attribute the analgesic effect of tonic SCS on the SNI model to the activation of large A $\beta$  dorsal column axons (supporting the GCT), as well as the electrochemical alteration of cell membranes and the involvement of neurotransmitters, receptors, and glial cells.

	<b>FDR <i>p</i>-value (increase/decrease)</b>	<b>Relevant Biological Processes Modulated by SCS in the SNI model</b>
Spinal Cord	0.063 (↑)	Inflammatory response; Immune related
	0.097 (↓)	Ion channel regulation (Voltage gated); Generation of neurons; synaptic transmission
	0.057 (↓)	Vesicle transport; regulation of calcium ion
	0.064 (↓)	Cell growth; cell activity pathways such as MAPKK, JUN kinase
	0.011 (↑)	Ribosomal proteins, 50% unknown proteins
	0.069 (↓)	Ion transport (cation and anion); GABA signaling, neuron development
	0.011 (↓)	Transmembrane/transporter activity, mostly ion transport; proton transport
	0.011 (↓)	Cell regulation changes; neuron differentiation and development
	0.016 (↑)	Activation of immune response
Dorsal Root Ganglion	0.012 (↓)	Ion transmembrane transport
	0.012 (↓)	Mitochondrial respiratory chain; regulation of superoxide, mechano-sensory perception of pain
	0.009 (↑)	Inflammatory response: cytokine and apoptosis regulation; Immune response to stimulus
	0.009 (↑)	Innate immune response; Adaptive immune response
	0.009 (↑)	Regulation of immune response: T-cell activation and differentiation
	0.074 (↑)	Histone acetylation; regulation of neuron migration; regulation of rho GTPase activity
	0.018 (↑)	Cell adhesion; cell development, wound healing
	0.086 (↓)	Calcium ion transmembrane transport
	0.062 (↑)	Cell development; extracellular matrix organization

**Table 1.**

*Gene ontology biological processes modulated in the ipsilateral dorsal quadrant of the spinal cord (directly under the electrode) and ipsilateral L5 dorsal root ganglion demonstrating molecular changes caused by SCS therapy with the SNI model. Relevant processes obtained after WGCNA and gene ontology analyses performed on microarray results. Only modules with significant False Discovery Rate (FDR) *p*-values are shown. Data from reference [44].*

Previously, this group looked at frequency-dependent outcomes of SCS, particularly regarding opioid receptors [47] and glial cell activation with SCS [48]. In the opioid receptor study [47], SNI-induced rats were administered naloxone or naltrindole (both opioid antagonists), or were made morphine tolerant. Rats then received SCS at 4 Hz, 60 Hz, or no SCS daily for 6-hour periods, lasting 4 days for each treatment. Testing for mechanical allodynia, they found naloxone prevented the analgesic effect produced by 4 Hz and 60 Hz stimulation, though a higher dose was required to block the effect of 60 Hz. Interestingly, naltrindole had no effect on 4 Hz SCS, but successfully impeded the effect of 60 Hz SCS. When testing the morphine-tolerant rats, they found that 4 Hz SCS did not have the same analgesic effect that it did in normal rats, while 60 Hz stimulation remained efficacious. This work resulted in the understanding that the frequency of SCS may determine the mechanism by which pain relief is achieved, and in this case, engaging different opioid receptors.

Glial activation, via immunohistochemical staining with known markers (GFAP, MCP-1, and OX-42), was measured in a separate study using 30-minute and 6-hour SCS durations and varying the intensity (as percent of the MT) [48]. Two weeks after the SNI was induced, mechanical hypersensitivity increased, as expected, as well as glial cell activity. The results indicated that withdrawal thresholds were positively correlated with increasing SCS duration (6 h vs 30 min) and by stimulating at higher intensities (90% vs 75% vs 50% MT). Glial cell activation was significantly decreased in both 4 and 60 Hz SCS, delivered for 6 hours at 90% MT.

Additional studies focused on the question of frequency importance in SCS, utilizing the SNI as a pain model. Song et al. investigated conventional 50 Hz (200  $\mu$ s PW, 80% MT) SCS compared to high frequency (HF) SCS at lower intensity (500, 1000, and 10000 Hz; 24  $\mu$ s PW, 40–50% MT) [49]. A miniaturized 4-electrode plate lead was implanted into the epidural space of the T13 vertebral level. Performing behavioral testing for mechanical hypersensitivity (von Frey filaments) and thermal hypersensitivity (ethyl chloride spray for cold, modified Hargreaves test for heat), they found no significant difference in the overall analgesic effect of conventional SCS versus SCS at higher frequencies. They did, however, find that conventional SCS had significant effect on increasing the gracile nucleus neuron discharge rate. HF SCS had no effect whatsoever. These results suggest that conventional and HF SCS have different mechanisms of action.

Building on the idea that SCS can be designed to modulate neuron-glial interactions, Vallejo et al. [50] utilized the SNI model with continuous SCS to evaluate a differential target multiplexed programming (DTMP) approach compared to high rate and low rate SCS. The DTMP approach utilizes multiple signals that are intended to target neuron and glial cells differentially. It was found that all SCS treatments resulted in significant reduction of mechanical hypersensitivity, but the DTMP approach provided more significant improvement as well as reduced thermal hypersensitivity (hot/cold plate test) after 48 hours of continuous stimulation. RNA-sequencing was performed to confirm the phenotypes. **Figure 3** provides a heatmap illustrating the significant effect of DTMP on sets of genes (modules) with similar expression patterns obtained through a Weighted Gene Co-expression Network Analysis (WGCNA) showing that the effect of DTMP SCS correlated stronger with the expression patterns of modules in naïve rats, compared to the pattern of untreated animals (No-SCS). In a follow up study, Cedeño et al. [51] demonstrated that the DTMP approach modulated neurons and glial cells (microglia, astrocytes, and oligodendrocytes) in a differential manner by using set of genes that were uniquely expressed (cell-specific transcriptomes) by each of the type of neural cell. The effect of DTMP on each of these cell-specific transcriptomes correlated strongly with the expression pattern of naïve animals, indicating a return of gene expression toward the state of naïve (healthy) animals.

### **2.3 SCS in the spinal nerve ligation model**

The spinal nerve ligation model (SNL) is one of the most popular preclinical models of neuropathic pain due to its reproducibility and lack of autotomy. During the surgery, initially described by Kim and Chung [52], the L5 spinal nerve is ligated with a 6-0 silk suture at a point just distal to the dorsal root ganglion (DRG), and cut distally, after the removal of the paraspinal muscles at the level of the L5 spinous process down to the sacrum, and the removal of the L6 transverse process.

Since the introduction of paresthesia-free stimulation parameters in the clinical setting, questions were raised on the value of the GCT as a practical construction to generate models to optimize SCS parameters. To find answers to some of these questions, Guan and coworkers have used the SNL model [53] to understand the specific

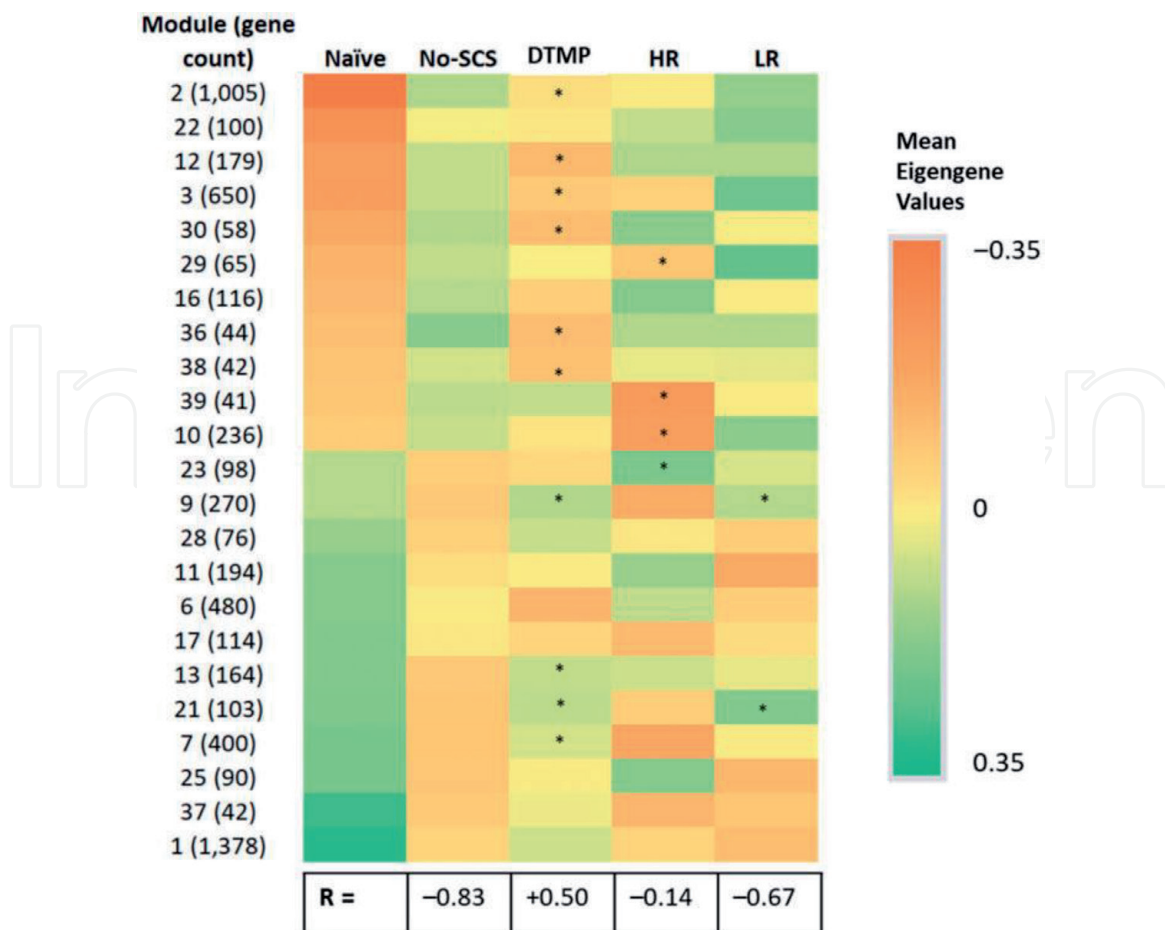


**Figure 3.** Heat map of mean module eigengene values for modules with significantly different comparisons ( $FDR-p < 0.2$ ) between SNI untreated animals (No-SCS) and naïve animals. A total of 23 modules out of the total 39 are affected. Asterisks (\*) indicate significantly different module eigengene values when comparing the SCS treatment to untreated animals (No-SCS).  $R$  is the Pearson coefficient for the correlation between eigengene values for naïve and each of the other groups. A negative value indicates an opposite trend. DTMP: differential target multiplexed programming; LR: low rate; HR: high rate; SCS: spinal cord stimulation. Reproduced from reference [50].

effects of different components of the electrical signals in SCS treatment. Before paresthesia-free SCS, common frequencies used in clinical and animal models ranged from 50 to 60 Hz, since referred to as conventional SCS. Due to the lack of agreement regarding the optimal frequency and stimulation intensity to maximize analgesia, these authors hypothesized that kilohertz-level SCS and conventional 50Hz SCS might differently activate gate-control mechanisms and affect peripheral afferent conduction properties [53].

Using the SNL rodent model of neuropathic pain, the authors evaluated intensity-dependent (20%, 40%, and 80% MT) pain inhibition of SCS at various frequencies (50 Hz, 1 kHz, and 10 kHz) while maintaining the PW constant (24  $\mu$ s). They further compared the effects of conditioning stimulation of the dorsal column, the primary structure targeted by SCS, at 50 Hz and 1 kHz on the conduction property of afferent A $\alpha$ / $\beta$ -fibers and inhibition of dorsal horn wide dynamic range (WDR) neuronal responses.

In their experiments, Guan and coworkers [53] advanced a custom-made quadripolar epidural SCS electrode up to the T10-12 spinal levels, via a small laminectomy at the level of T13. Mechanical hypersensitivity was assessed by determining the PWT using von Frey filaments. To further evaluate clinical conditions in the SNL model, the authors choose stimulation intensities set at either 20%, 40%, or 80% of the MT to test the effect of the described frequencies on pain-like behavior.

Stimulation was conducted for 30 mins on days 12, 13, and 14 (week 1) and days 19, 20, and 21 (week 2) post-SNL. Behavioral testing was done at time 0, 15 (within the activation of SCS), 30 (end of stimulation), and 60 min. A cross-over design was implemented to avoid the order effect while switching the different frequencies.

Interestingly, rats exposed to 10 kHz SCS at 80% MT often exhibited signs of discomfort. For comparison, a small number of animals were implanted, but not stimulated, and served as a stimulation sham. When stimulation was applied at 20% MT, the effect was marginal for all the tested frequencies. The average mean PWT across the three treatment days was increased from the pre-stimulation level in all SCS groups but was statistically significantly higher than that of sham stimulation only in the 1 kHz and 10 kHz groups. Notably, there was a trend for SCS induced inhibition to increase gradually from the first to the third treatment in all groups. When using 80% MT the mean PWT was significantly increased from the first day of stimulation in both the 1 kHz and the 10kHz SCS groups. Of notice, the mean PWT in the 1 kHz and 10 kHz were both higher than that of the 50 Hz group on the first day of stimulation. The inhibitory effect of 50 Hz stimulation increased progressively during the second and third days of stimulation. The authors concluded that the SCS analgesia in SNL rats depends on both intensity and frequency, and high-intensity kilohertz level SCS provides earlier inhibition of mechanical hypersensitivity than conventional 50 Hz SCS. These results imply that analgesia from kilohertz and 50 Hz SCS may involve different mechanisms.

In a follow-up report, Guan and coworkers [54] explored how charge delivery affects pain inhibition by different frequencies at intensities that seem to be below the sensory threshold (40% MT), and which component of stimulation runs the therapeutic actions. Epidural electrodes were implanted 5 to 7 days post-SNL, in a similar fashion described by this group previously [53]. Based on the frequency, PW, and intensity, the authors calculated the charge-per-pulse, duty time, and charge-per-second. Then, four patterns of high-dose subthreshold active recharge biphasic signals at different frequencies with similar duty times were produced by adjusting the PW (200 Hz with 1 ms PW, 500 Hz with 0.5 ms PW, 1.2 kHz with 0.2 ms PW, and 10 kHz with 0.024 ms PW). Finally, the authors included one 50 Hz with 0.2 ms PW at subthreshold and a sham (no SCS) group. Because clinical and animal data suggest that subthreshold SCS may have a slower onset, stimulation was carried for 120 mins (one session per day) from days 14 to 17 (week 1). The behavioral response was determined by measuring the PWT 30 mins pre-SCS, at 0, 30, and 60 mins during SCS, and 0, 30, and 60 mins post-SCS to evaluate carry-over effects. In those groups that showed increased tolerance to mechanical hypersensitivity, the peak effect appeared at 60 to 90 mins after initiation of SCS and faded shortly after the stimulation was completed. The onset of significant PWT increase was observed from day one in the 200 Hz and 10 kHz groups and was observed on day two in the 1.2 kHz group. Although 200 Hz SCS had the longest PW, the highest charge-per-pulse and the lowest charge-per-second, and 10 kHz had the shortest PW, the lowest charge-per-pulse, and the highest amplitude and charge-per-second, the two groups provided comparable improvements in PWT. These findings suggest that the efficacy of the inhibitory effect is not correlated to the difference in individual SCS parameters (frequency, PW) but is positively correlated with the electrical dose. Probably, the most interesting finding is that at subthreshold SCS amplitudes, mechanical hypersensitivity was not only inhibited by 10 kHz but also at lower frequencies (200 Hz). The authors concluded that using low-frequency subthreshold SCS and longer PWs, could be a more energy-efficient stimulation paradigm for inhibition of mechanical hypersensitivity when compared with 10 kHz SCS.

## 2.4 SCS in a chemotherapy-induced neuropathic pain model

The administration of chemotherapy agents for the treatment of cancer often results in the onset of neuropathic pain due to peripheral nerve damage. Recently, Sivanesan et al. [55] reported on the efficacy of SCS in reducing mechanical and thermal hypersensitivity in a rodent model of chemotherapy-induced peripheral neuropathy (CIPN). The chemotherapeutic paclitaxel (PTX), common in the treatment of ovarian, breast, and lung cancers, can induce painful peripheral neuropathy even at therapeutic dosages. Often this pain is severe enough to necessitate a reduced dose of PTX and persists after cessation of the drug in nearly a third of cases. Other chemotherapeutic agents, including platinum-based agents, and proteasome inhibitors like bortezomib, are also known to induce similar neuropathies [56].

Induction of the model began by acclimation of a group of adult male rats that were divided into three groups: (1) SCS + PTX, (2) PTX, or (3) naïve. Behavioral testing consisted of assessments of mechanical hypersensitivity (von Frey filaments) and thermal hypersensitivity (via dry ice application) of the hind paws.

Animals assigned to receive SCS underwent a T13 laminectomy and were implanted with a quadripolar miniaturized lead in the dorsal epidural space corresponding to the T13-L1 spinal cord. Stimulation parameters were set to conventional settings with 50 Hz frequency, 0.2 ms PW, and current intensity at 80% MT. Subsequently, animals in the PTX and SCS + PTX groups were administered 1-2 mg/kg PTX, via intraperitoneal (i.p.) injection, every other day for four days. Naïve animals received i.p. injections of the vehicle used in the PTX groups. SCS was administered daily for 6-8 hours over the course of two weeks. To substantiate whether SCS can avert the development of CIPN, PTX was administered at the same time as the stimulation. Implanted animals that did not receive SCS treatment were included as control animals.

Rats developed hypersensitivity one week after the first administration of PTX that was sustained for 25 days. Interestingly, early administration of SCS attenuated the development of mechanical hypersensitivity associated with neuropathic pain-like behavior induced by administration of PTX (**Figure 4**). SCS did not fully recover to the PWT in naïve animals, but the preemptive effect of SCS is noteworthy. Early application of SCS also prevented the development of cold hypersensitivity. It is also important to note that the analgesic effect of SCS persisted for at least 2 weeks after stopping SCS treatment.

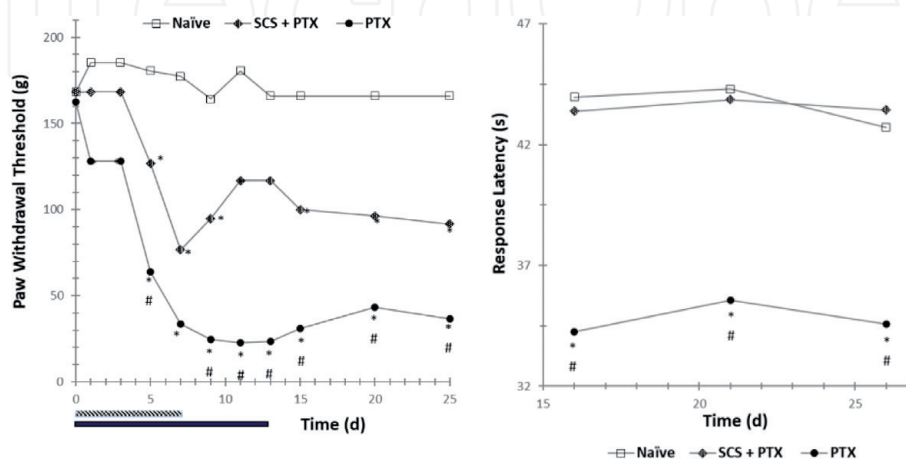


**Figure 4.** Mechanical hypersensitivity (left) and cold thermal hypersensitivity (right) of animals treated with SCS (SCS + PTX), untreated (PTX) and naïve. The patterned box indicates the time of PTX administration. The black box indicates the time of SCS administration. \* indicates significant differences ( $p < 0.05$ ) relative to naïve, # indicates significant differences ( $p < 0.05$ ) relative to PTX + SCS. Values obtained from reference [55].

L3-L6 spinal cord tissue was harvested 17 days after SCS was applied, and RNA in the samples was sequenced to investigate changes in gene expression and biological processes of treated, untreated, and naïve animals. It was found that some genes associated with mechanosensation, neuroimmune response, and glial activation were affected by the CIPN model. The authors hypothesized that repetitive dosing of SCS increased the expression of genes that enhance adenosine-related activity, which has been shown to enhance pain inhibition by SCS when using the CCI model [14]. The authors also observed that SCS downregulated GABA reuptake-related genes, which is consistent with a previous observation in rats after sciatic nerve injury [57]. They postulated that downregulation of genes such as *Gat3* (a GABA transporter expressed by glial cells) by SCS may increase GABAergic signaling that inhibits neurotransmission in CIPN rats. The GABAergic inhibition of excitatory neurotransmitters may involve then the suppression of calcium influx into presynaptic terminals, which is regulated by astrocytes.

## 2.5 SCS in a model of painful diabetic neuropathy

Originally developed in the early 1960's for studying diabetes mellitus, the streptozotocin (STZ)-based painful diabetic neuropathy model (SPDN) uses an antibiotic derived from *Streptomyces achromogenes* to selectively kill insulin secreting  $\beta$ -cells in the pancreas [58]. The results replicate symptoms seen in type 1 diabetes including dysregulation of blood glucose, decreased body weight, and peripheral artery disease leading to painful diabetic neuropathy.

Early investigations with this model to study the effects of SCS were conducted by Wu et al. [59] to explore the effect of SCS on blood flow in the periphery. Adult male rats were divided into two groups: (1) diabetic rats and (2) non-diabetic rats. Diabetic rats were injected with 50 mg/kg streptozotocin i.p., while the non-diabetic animals were injected with an equivalent volume of vehicle (citrate buffer). Animals were monitored weekly for weight loss and blood glucose levels. After four weeks, animals were tested for vasodilation in response to SCS provided via a spring-loaded unipolar ball electrode placed on the right or left side of the subdural face of the dorsal columns at the L2-L3 spinal segments. SCS was set to 50 Hz frequency, 0.2 ms PW, with monophasic rectangular pulses. Current was applied for 2 minutes at 30, 60, or 90% of the MT. It was found that MT in diabetic rats was significantly higher than in non-diabetic rats, and that SCS at the largest intensity attenuated SCS-induced vasodilation in diabetic rats. Furthermore, increasing SCS from 30% to 90% of MT increased blood flow in non-diabetic rats but not in diabetic rats. The study suggested that SCS-induced vasodilation improves peripheral blood flow, although this seems partially impaired in the diabetic animals.

In a later study, van Beek et al. [60] utilized the SPDN model to explore the effect of increasing the stimulation frequency on mechanical hypersensitivity induced by the model. In this study the dosage of STZ was increased to 65 mg/kg, to ensure the development of type-1 diabetes in four days instead of four weeks. Animals were implanted with a quadripolar lead via a T13 laminectomy into the dorsal epidural space of the T10-T12 spinal cord. Stimulation parameters were set to 200  $\mu$ s PW, intensity at 67% MT and frequency at either 5, 50, or 500 Hz. Sham-stimulated animals were used as controls. SCS sessions were 40 minutes/day for four consecutive days. It was found that SCS at all frequencies alleviated mechanical sensitivity similarly, but stimulation at 500 Hz elicited a delayed response.

In other study, van Beek et al. [61] utilized the SPDN model to evaluate the long-term efficacy (10 weeks) of conventional SCS treatment. As before, the SPDN model was induced in male rats using an i.p. injection of 65 mg/kg STZ. Animals were monitored for weight loss and blood glucose to establish response to the model.

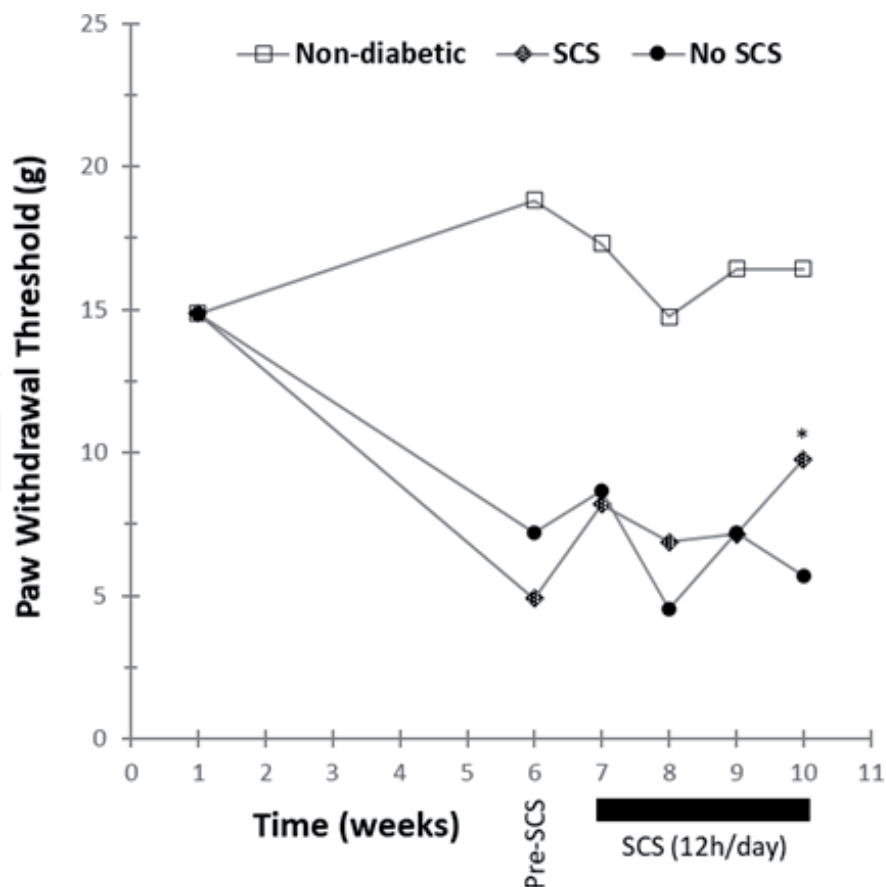


**Figure 5.** Effect of conventional SCS on mechanical hypersensitivity in a diabetic neuropathic pain model. \* indicates a significant difference ( $p < 0.05$ ) relative to No-SCS. Values obtained from reference [61].

An internally implanted pulse generator fitted with a quadripolar lead was required due the longer duration of the study. The quadripolar lead was implanted via a L1 laminectomy into the dorsal epidural space of the L2-L5 spinal cord. Stimulation parameters were 50 Hz frequency, 210  $\mu$ s PW, intensity at 67% of the MT, 12 h/day for four weeks. A group of implanted SPDN animals sham for SCS were included as a control. The results indicate that long-term conventional SCS decreases mechanical hypersensitivity even after cessation of SCS in the SPDN model (Figure 5).

### 3. Animal models of SCS for inflammatory pain

The injection of a chemical inflammatory agent in a skin dermatome has been effectively used for the study of the mechanism of acute and persistent inflammatory pain [62]. Such agents include solutions of formalin, complete Freund's adjuvant, or carrageenan (CAR). The CAR model has been adapted to study the effect of SCS in inflammatory pain in the limbs of rodents. Cui et al. [63] reported the first account of the utilization of a carrageenan-based model of chronic nociceptive pain coupled to SCS. The pain model was adapted from Woolf and Doubell [64] and consisted of the injection, under standard halothane anesthesia, of 0.15 mL solution of carrageenan lambda (in 0.9% saline to a concentration of 1%) in the mid plantar part of the hind paw. The inflammatory agent induces an edema at the site of injection and decreases the threshold for paw withdrawal or vocalization to mechanical stimuli in the affected area. Adult male Sprague-Dawley rats epidurally implanted, under anesthesia, with a monopolar cathode ( $2 \times 3 \text{ mm}^2$ ) placed retrograde in the L1-L3 vertebral region via a laminectomy in T11. The anode was placed subcutaneously in

the supravertebral region adjacent to the cathode. Rats were allowed to recover for 3 days post-surgery before any experimentation. Current-controlled SCS was applied using a pulsed signal with a width of 200  $\mu$ s at a frequency of 50 Hz. The intensity was set to 67% of the MT and was on average 1.0 ( $\pm$  0.3) mA. These parameters correspond to those used clinically during conventional SCS therapy. Treatment was applied for 30 minutes at 3 h, 1, 3, 5, 7 and 9 days after injection of the CAR solution. SCS was also applied to another group of animals 3 days (30 minutes/day) before injection besides the timepoints after injection. The study also included control animals that were injected with CAR but were not implanted with the SCS system, and animals that were subjected to SCS but were not injected with CAR. The extent of local inflammation was determined by measuring the circumference of the metatarsal region and mechanical sensitivity was measured by recording paw withdrawal or vocalization upon applying pressure to the affected paw. A pressure gauge measured the force (in g) that elicited the withdrawal or vocalization response.

The mean circumference of the edema at the paw was around 30 mm before injection (no edema) and increased to a maximum at around 43 mm 3 hours after injection. The edema gradually decreased back to baseline at day 7-9 post-injection. The mean paw withdrawal/vocalization threshold was 215-220 g before CAR injection and decreased to 77 g at 3 hour after CAR injection. Mechanical hypersensitivity reduced gradually and reached baseline at around day 7 post-injection. The reduction in mechanical hypersensitivity correlated well with the reduction in the edema (**Figure 6**). The application of 30 min of SCS at every time point produced a significant increase of the size of the edema until day 5 post-injection (**Figure 7**). However, mechanical sensitivity was only significantly increased by SCS at the 3h point after CAR injection. At day 3, mechanical sensitivity was reduced significantly relative to the pre-stimulation value and was similar at days 7 and 9 post-injection. Authors reported that application of SCS pre-emptively did not provide a beneficial effect. Application of SCS in the absence of the inflammatory insult did not produce significant changes in circumference size and mechanical sensitivity.

Authors concluded that this model is a representation of subacute pain between the third day post CAR injection and the 14th day, which is concomitant to the invasion of different types of inflammatory cells, while the stage previous to the

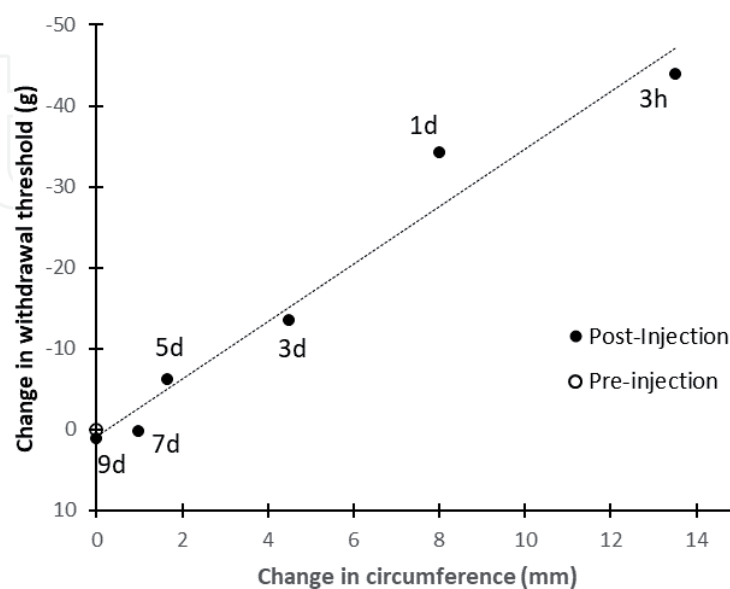


**Figure 6.**

*Correlation between edema size resulting from CAR injection as measured by the mean circumference of the metatarsal level of the paw and the change in the threshold force (g) that elicits paw withdrawal or vocalization. Labels by every post-injection point indicates the time point. The values at days 7 (7d) and 9 (9d) post-injection are the same as the pre-injection values. Values obtained from reference [63].*

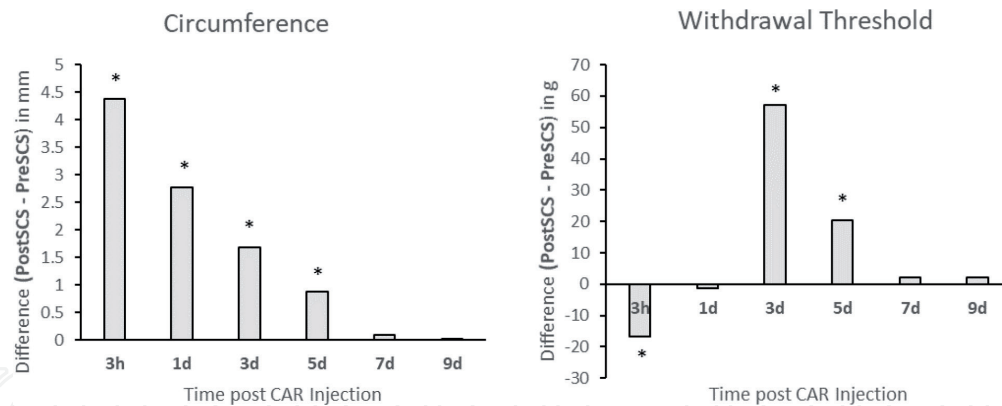


**Figure 7.** Change in the edema size (left) and mechanical hypersensitivity (right) as a result of 30 minutes/day of SCS. A positive change in withdrawal threshold is equivalent to a reduction in hypersensitivity. \* indicates a significant difference ( $p < 0.05$ ). Values obtained from reference [63].

third day post-injection represents an acute pain phase. It was surprising to observe that the SCS signal applied in this study increased the size of the edema as well as mechanical sensitivity in the early stage of the acute phase. However, the increase in hypersensitivity was not likely causal to the edema, and rather may be due to plasticity changes in the dorsal horn as a result of the stimulating signal and the acute inflammatory process. Once the inflammatory processes have settled in during the subacute phase, authors hypothesized that SCS provides an analgesic effect due to the inhibition of neuronal hyperexcitability due to A fiber-mediated wind up.

Years later, the same group reported [49] on using the CAR-based inflammatory pain model to assess the effect of signal rate at low intensities in the acute stage of the model. This was motivated by a shift in SCS paradigm resulting from the clinical introduction of a SCS therapy that provided pain relief at intensities below the perception threshold, thus removing the need for paresthesia overlap of the painful dermatome required by conventional SCS which operates at low frequency (50 Hz), in contrast to the high frequency (10 kHz) used by the novel therapy. The authors utilized signals at 50 Hz (conventional frequency), and 10 kHz, which is referred to as high frequency SCS (HF SCS). In the same report, the authors also studied the effects on HF SCS (500 Hz, 1 kHz, and 10 kHz) on the SNI model, which was allowed to develop more chronically (2 weeks after nerve injury) before SCS intervention. In this work, authors used male adult Wistar rats, which were injected with 0.15 mL of a 1% saline solution of CAR in the hind paw as previously described [63]. Animals were implanted with a SCS system consisting of a paddle lead with four circular poles (0.9-1.0 mm diameter) spaced by 1.8-2.0 mm, which was introduced epidurally via laminectomy at the T13 vertebral level and placed anterograde to cover the T10-T12 levels. This was a variation from the previous report [63]. Animals were left to recover from surgery for 48 hours before any additional experimental intervention. Pain-like behavior was tested before injection (baseline, before stimulation and after 120 minutes of SCS at days 1, 2 and 3 after CAR injection. The test consisted of applying force progressively with clamping forceps (algometer) terminated in a blunt tip in the affected paw until the animal withdraws the paw. The algometer was equipped with a pressure gauge that reads the force exerted (in g) at the threshold of paw withdrawal. In contrast to the previous study by this group, the circumference of the metatarsal level of the paw was not measured, so the effect of SCS frequency on the edema was not determined. SCS was distributed to the four contacts in the paddle lead using adjacent bipoles (+--+ , rostral to caudal). Conventional SCS (50 Hz) used monophasic pulses 200  $\mu$ s wide and current-controlled intensity set to 80% of the MT, corresponding to intensities

in the 0.48 to 0.64 mA range. The HF-SCS (10 kHz) monophasic pulses were 24  $\mu$ s wide with intensities set in the range 0.3-0.4 mA, which correspond to 40-50% of the MT, which were defined as subparesthetic based on observation of behavioral responses. Untreated animals served as control. Mean paw withdrawal threshold was 72 g before injection and decreased to around 19 g 1 day after CAR injection. As expected, for this model, the mean withdrawal threshold gradually increased reaching around 30 g and 56 g at days 2 and 3 post-injection, respectively (**Figure 8**).

Neither conventional SCS nor HF-SCS provided a significant improvement of acute inflammatory pain over the course of 3 days, although it is worth mentioning that, in contrast, their previous work reported a significant difference at 3 days post CAR injection. The authors did not comment on their counter results, but it is plausible that the position of the lead, which was reported to be a differing factor may have influenced the outcome. A lumbar location may modulate neural circuits of the hind paw more effectively than a thoracic location used in this study. The findings for the acute inflammatory pain were similar to what was found when healthy animals were subjected to SCS and a test of acute pain (pinch force with a pointy tip in the algometer), but in contrast to the results observed in the neuropathic chronic pain model, in which 120 minutes of both conventional and HF-SCS treatments reduced mechanical hypersensitivity significantly. Thus, it can be concluded from the study that neither HF-SCS nor conventional SCS provide relief from acute inflammatory pain (as well as acute nociceptive pain), in agreement with previous clinical and well-controlled observations [65–67] and had led to the establishment of a segmental mechanism of action in which SCS works by modulating conduction of dorsal column fibers within a particular segmental circuitry that has reached

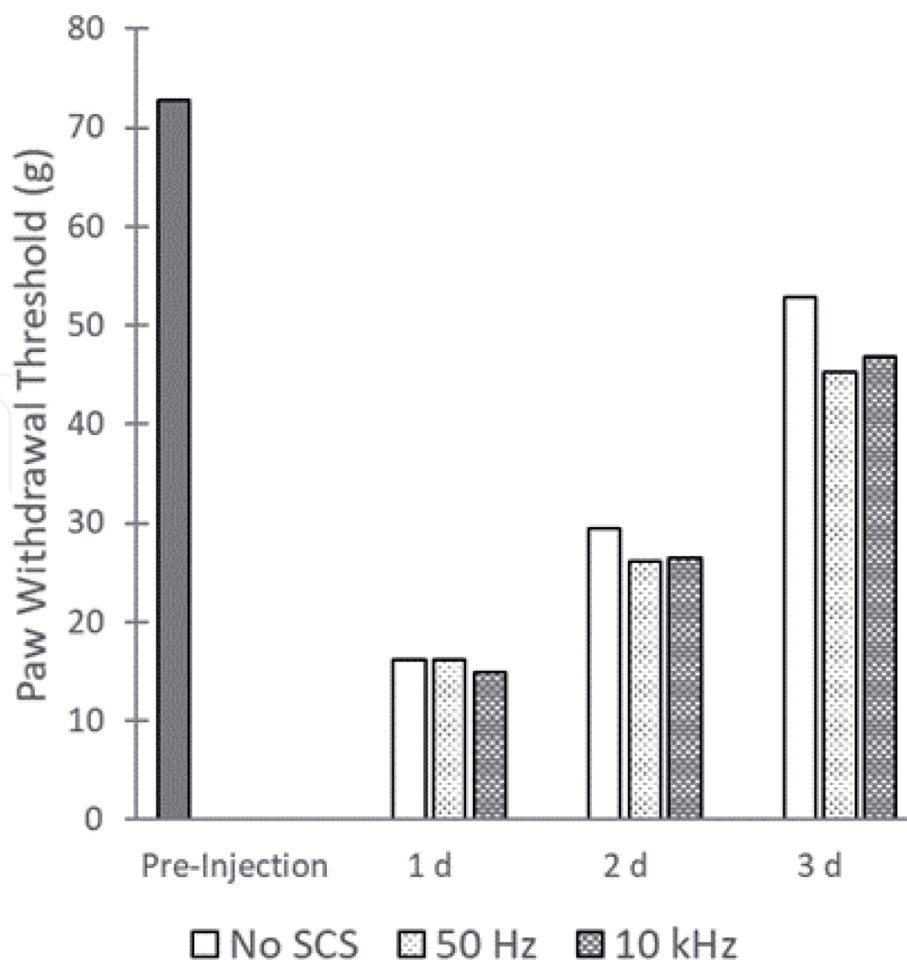


**Figure 8.** Effect of SCS treatments on acute inflammatory pain. Values obtained from reference [49].

a level of central sensitization during the establishment of chronic pain due to a peripheral injury, such as in the SNI model of neuropathic pain tested.

Recently, Sato et al. [46] reported the utilization of a CAR-based model to study the effect of conventional SCS on joint inflammatory pain. This group had previously found [68] that the unilateral intraarticular anterior injection of 0.1 mL of a 3% solution of lambda carrageenan (type IV, dissolved in 0.9% saline) into the left knee joint of rats induces pain-like behavior that manifests as increased thermal (hot) and mechanical hyperalgesia in the ipsilateral hind paw and knee. The model can be used to evaluate acute or chronic onset of inflammatory pain. In their recent work, they implemented this joint inflammatory pain model to test the effect of short doses (15 min/day) of conventional SCS (60 Hz, 250  $\mu$ s PW, intensity at 90% of the MT) on thermal and mechanical hyperalgesia using an acute stage of the model. The SCS system had been previously described [48, 69] and consisted of a stimulation lead epidurally introduced, under anesthesia, via laminectomy at the T13 vertebral level and positioned rostrally. The authors did not provide details on the lead design and final position of it relative to spinal levels within the epidural space. Lead wires were tunneled to an internal neurostimulator (Interstim iCon, model 3058, Medtronic Inc., Minneapolis, MN) implanted subcutaneously in the left flank. This allowed animals to roam freely in their cages while being stimulated. Animals were tested for both paw and knee withdrawal to noxious mechanical stimuli before CAR injection, and 30 min before and after SCS (15 min) on days 1, 2, 3, and 4 after injection. Paw withdrawal thresholds were obtained using von Frey filaments with bending force in the range 1-402 mN applied to the plantar surface of the paw ipsilateral to the affected joint. Measurements in the contralateral paw served as internal controls. Knee withdrawal thresholds were measured by compressing the affected extended knee with a pair of calibrated forceps (30 mm<sup>2</sup> tip) until the knee was withdrawn due to the applied force. Mean paw and knee withdrawal thresholds are shown in **Figure 9**.

An acute application of conventional SCS, as applied in this work, improved mean withdrawal thresholds significantly relative to the pre-SCS state, implying that conventional SCS may be used to treat acute inflammatory pain. The study did not address the effects of a chronic inflammatory state, which is achievable with this CRA model. Similar to what was reported for effects on the SNI neuropathic pain model, the effect is reversible and reproducible over the different days of treatment. It has been established that SCS modulates inflammatory processes in the stimulated area of the spinal cord that contain neural circuits associated with the painful areas. These

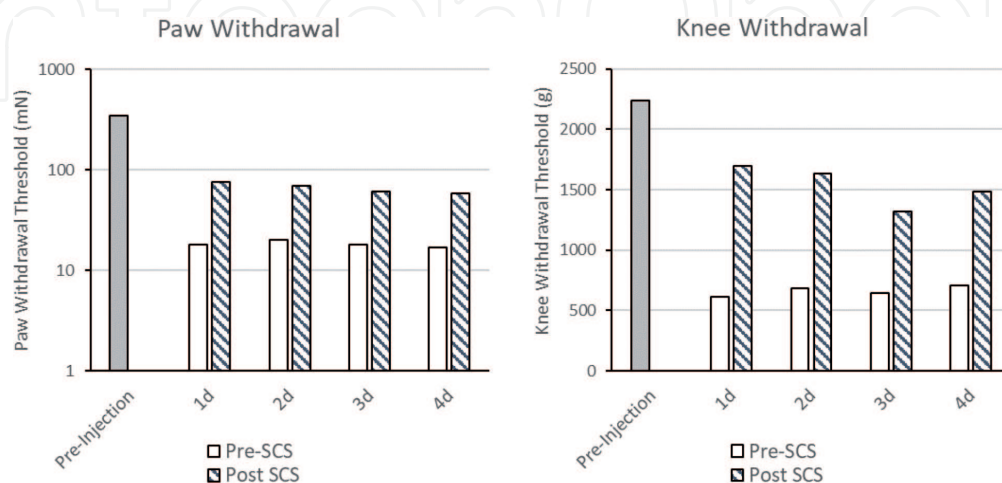


**Figure 9.** Effect of SCS treatments on acute inflammatory joint pain as reflected in the ipsilateral paw and knee. All post-SCS values are significantly increased ( $p < 0.05$ ) relative to Pre-SCS values. Pre-SCS values are significantly reduced relative to pre-injection. There is no significant difference between treatment days. Values obtained from reference [46].

neural circuits contain neurons and other abundant non-neuronal cells that are highly involved in the establishment and chronification of pain, even at early stages. It is quite interesting to note that the effect of SCS sets in as early as 1 day to alleviate hyperalgesia associated with acute knee inflammation, which was not observed by Linderoth and coworkers when inflammation was elicited in the hind paw [49, 63]. It is plausible that the circuits operating in the thoracic region for inflammation of the hind paw are not as effective for SCS, in contrast to treat inflammation of the knee joint.

#### **4. Animal models of SCS for ischemic pain**

It has been established that SCS modulates vasodilation in the lower limbs and feet dermatomes associated with vertebral segments being stimulated [70]. This has justified SCS as an alternative treatment for nociceptive pain and associated symptoms related to advanced cases of peripheral arterial occlusion disease (PAOD), which leads to ischemia and the subsequent neuropathy due to the lack of blood supply to nerve terminals. Other clinical uses of SCS related to vasodilation modulation include Rynaud's syndrome and angina pectoris. In the absence of a pain model related to PAOD, animal models that measure the modulation of blood flow and vasodilation have been used to demonstrate the mechanism of action of SCS treatment of peripheral vascular diseases. Although there is no evidence that SCS is effective on acute nociceptive pain, the modulation of vasodilation is hypothesized as the mechanism of action for relieving ischemic conditions and recover the flow of nutrients into the affected nerve terminals. Linderoth and Foreman's groups have collaborated to measure the effect of low rate SCS on blood flow changes in the skin dermatomes of the hind paws of anesthetized rats. In one experiment [71], a spring-loaded monopolar ball cathode was placed in the subdural surface of the L1-L3 dorsal columns (left or right) of anesthetized rats to assess the role of SCS in modulating the sympathetic autonomous system. SCS monophasic pulses (50 Hz, 200  $\mu$ s PW, 66% of the MT) were applied for 2 minutes. Blood flow was monitored using laser-based doppler probes placed in the glabrous surfaces of the hind paws ipsilateral and contralateral to the stimulation. Another group of animals was subjected to total sympathectomy, while the other was subjected to the ganglionic transmission blocker hexamethonium. In a separate experiment [72], the effect of SCS on the sympathetic nervous system was determined by evaluating the role of ganglionic transmission (with hexamethonium blockade), alpha-adrenergic receptors (phentolamine or prazosin blockade), beta-adrenergic receptors (propranolol blockade), and adrenal catecholamine secretion (adrenal demedullation) in paralyzed anesthetized animals. The left L1-L2 vertebral region was stimulated epidurally with a monopolar ball cathode (0.9 mm diameter) that delivered pulses at 50 Hz, 200  $\mu$ s PW, and 0.6 mA of intensity. Blood flow was monitored using laser Doppler probes in each hind paw. Although both studies concurred that SCS increases peripheral blood flow in the ipsilateral limb by about 200% concomitant to a reduction of flow resistance of ~50%, there were disagreements in the role of sympathetic contributions, which prompted the formulation of a second hypothesis involving the antidromic activation of the release of vasodilators, such as calcitonin gene-related peptide (CGRP) and nitric oxide. A further report [73] explored the effect of SCS pulse rate on blood flow, finding that pulsing at 500 Hz provided a significant increase of vasodilation relative to pulsing at 200 Hz and 50 Hz at similar pulse widths and intensities. The frequency effect seems to be related to increased release of CGRP, induced by activation of fibers containing the capsaicin receptor (TRPV-1). In conclusion, the reduction of nociceptive lower limb pain due to ischemia has been indirectly associated with SCS-induced vasodilation that provides an increase in blood flow and

the concomitant decrease of flow resistance in the affected limb. It is plausible that vasodilation is due to the release of agents CGRP and nitric oxide from the stimulated fiber afferents and at some extent by modulation of the sympathetic nervous system.

## 5. Translational equivalence of animal models

Besides rodent (mostly rat) models, there have been reports of SCS effects on ovine models of neuropathic pain. As presented in section 2.1 above, Reddy et al. [17] reported on the utilization of female sheep to develop a CCI model to study the effect of tonic SCS. The advantage of using a large animal model is that it provides a way to bridge the translation of SCS parameters toward clinical application for longer exposures in anatomical environments that are more similar to that of humans. These authors found that the model provided a significant reduction of mechanical hypersensitivity upon continuous SCS for one week. A closer examination of the

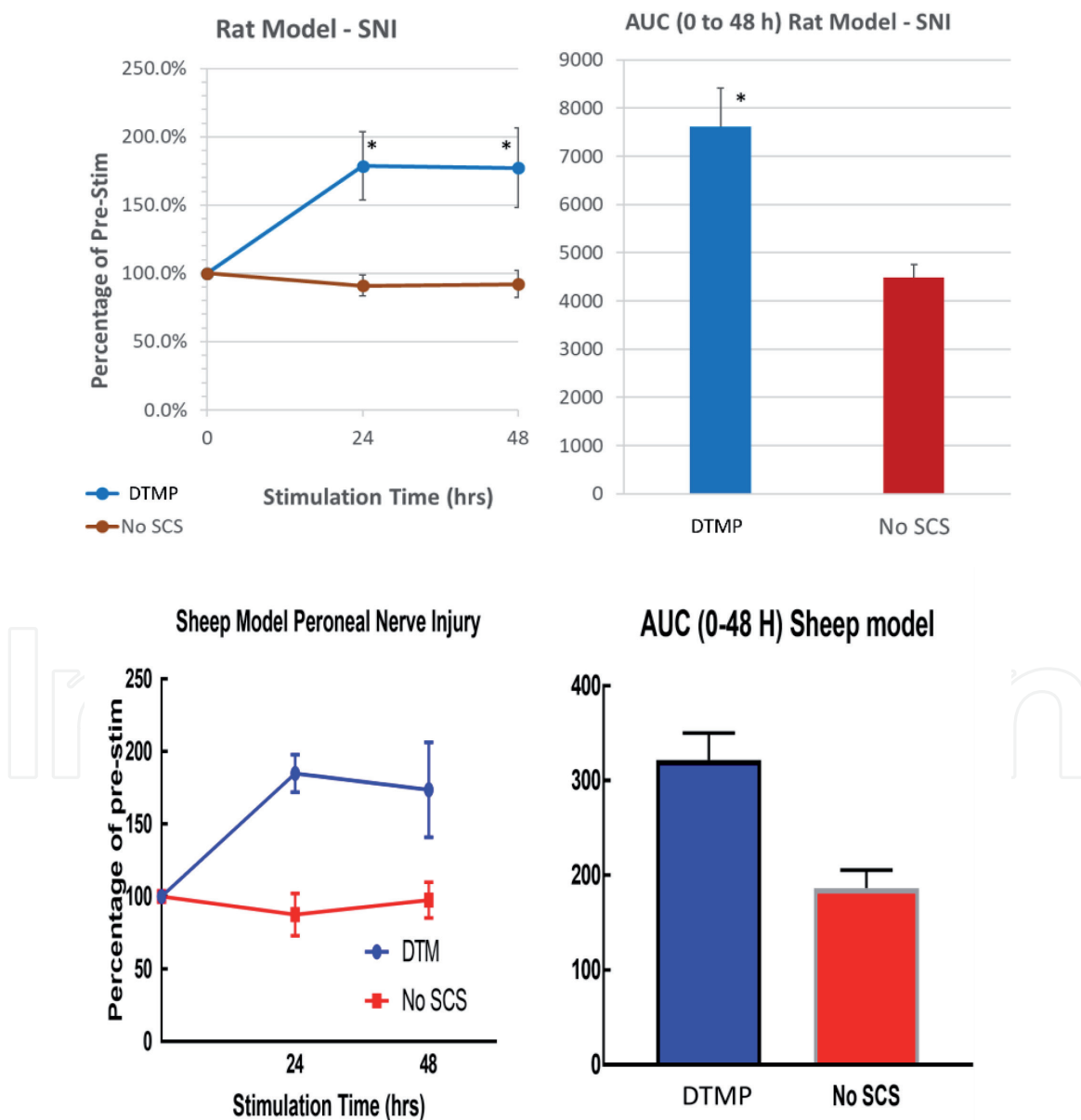


**Figure 10.** Top row: Mechanical hypersensitivity of rats subjected to SCS with a DTMP approach in comparison with untreated animals (No SCS) and corresponding areas under the curve (AUC). Bottom row: equivalent measurement obtained from sheep. \* denotes significant differences ( $p < 0.05$ ) between treated and untreated animals.

reported data for 5 animals, reveals that one of them was a non-responder to the pain model since there was not a decrease of the limb withdrawal threshold (WT). If data from this animal is discarded, the CCI model reduced the WT to a mean 51% ( $\pm 6\%$ ) relative to the mean WT of the control measurements in the contralateral limb. The mean WT of the responders after SCS corresponded to 85% ( $\pm 13\%$ ) of the mean WT of the control. This is consistent with the findings in rodents, although a direct comparison is not possible because there are not reports on rodent CCI models with continuous SCS.

Vallejo et al. [74] reported on a comparison of the effect of SCS based on the DTMP approach on a rat and sheep models after 24 and 48 h of continuous treatment. The pain model in the rats was the SNI as previously described [42, 43], while the sheep model is the equivalent peroneal nerve injury (PNI) developed by Wilkes et al. [75] and adapted for SCS by implanting a cylindrical octapolar human-grade lead (1.3 mm diameter) in the L1-L3 epidural space. DTMP consisted of multiplexing 4 pulsed signals with frequencies in the 50 Hz to 1.2 kHz and PW of 200  $\mu$ s at an intensity of 50% of the MT. Mechanical hypersensitivity was obtained before starting SCS, as well as at 24 h and 48 h of continuous SCS, using an electronic von Frey anesthesiometer. In order to compare rodent and ovine results, the WT were normalized to the pre-SCS values (**Figure 10**). Rodent data is for individual subjects (N = 13). Ovine data is from two sheep that were evaluated in a crossover experiment, in which one sheep was stimulated while the other one served as a No-SCS control. After a one-week break for washing out the effects of SCS, the animal that had not been treated was subjected to SCS while the other one was the No-SCS control. This process was repeated until obtaining a set of six measurements.

DTMP significantly relieved mechanical hypersensitivity in the rat model equivalent to 78.6% at 24h and 77.3% at 48 h in the rat model relative to the pre-SCS and No-SCS measurements. Similar effects were seen in the sheep model where the decrease in mechanical hypersensitivity was 84.8% at 24h and 73.7% at 48 h. These results demonstrate translational equivalence between two animal models of neuropathic pain for the first time.

## **6. Conclusion**

Certain limitations exist in the development of animal models that simulate human pathological conditions of pain. For instance, the most common clinical indication for SCS has become the treatment of intractable neuropathic pain of the lower back and legs, largely associated with failed surgical spine interventions (failed back surgery syndrome, FBSS), which causes axial back pain that radiates to the limbs in a unilateral or bilateral manner. The existing rat models of neuropathic pain, which are described in this chapter, are mostly peripherally induced (nerve injury) and test the manifestation of mechanical hypersensitivity in the paws, not necessarily in the leg of the animals. An animal model that resembles FBSS has yet to be developed. Such peripheral nerve injury models, however, resemble symptoms found in other pain-related syndromes such as complex regional pain syndrome (CRPS), which are also indicated for SCS treatment in humans. Despite these limitations, the existing models have proven extremely useful to understand the effects of various modalities of SCS on pain-like behavior of the animals, and more importantly, on the mechanistic understanding of SCS via the molecular analysis of samples obtained from neural tissues (spinal cord, DRG) that cannot be obtained in clinical assessments. Such molecular evaluations have made use of pharmacological approaches that use the coadministration of neurotransmitters agonists and antagonists, opioids, receptor blockers, etc., as well as immunohistochemical analysis

that target cellular markers of glial activation. Recent approaches are most robust and utilize high throughput transcriptomic and proteomic analysis in combination with many bioinformatic tools that provide an understanding of the effects of SCS on complex biological processes that involve a multitude of proteins and their encoding genes. These advancements should provide the field with tools to enhance current therapies and improvements on pain diagnostics that could ultimately lead to an integral and personalized treatment of painful conditions in humans. Animal models will continue to play a crucial role in the development of the science and technology of electrical neuromodulation for treating pain.

## Acknowledgements

The authors want to acknowledge our colleagues, Dana Tilley, William Smith, Ashim Gupta, Cynthia Cass, Maggie DeMaegd, Randi Wilson, Louis Vera-Portocarrero, Melanie Goodman-Keiser, Samuel Thomas, Alejandro Vallejo, and Tina Billstrom who have provided their help in developing our own SCS animal models.

## Conflict of interest

DLC and RV are consultants and scientific advisors for Medtronic Inc. They are also coinventors in patents related to differential target multiplexed (DTM) spinal cord stimulation.

## Author details

Joseph M. Williams<sup>1</sup>, Courtney A. Kelley<sup>1,2</sup>, Ricardo Vallejo<sup>1,2,3,4</sup>, David C. Platt<sup>1,2</sup> and David L. Cedeño<sup>1,2,3\*</sup>

1 Department of Psychology, Illinois Wesleyan University, Bloomington, USA

2 Lumbrera LLC, Bloomington, USA

3 SGX Medical LLC, Bloomington, USA

4 National Spine and Pain Center, Bloomington, USA

\*Address all correspondence to: [dclumbrera@gmail.com](mailto:dclumbrera@gmail.com)

## IntechOpen

© 2021 The Author(s). Licensee IntechOpen. This chapter is distributed under the terms of the Creative Commons Attribution License (<http://creativecommons.org/licenses/by/3.0>), which permits unrestricted use, distribution, and reproduction in any medium, provided the original work is properly cited. 

## References

- [1] Melzack R, Wall PD. Pain mechanisms: A new theory. *Science* 1965; 150: 971-979.
- [2] Köhler W. On unnoticed sensations and errors of judgment. *Sel Pap Wolfgang Köhler* 1971; 13-39.
- [3] Parpura V, Verkhratsky A. Homeostatic function of astrocytes: Ca<sup>2+</sup> and Na<sup>+</sup> signalling. *Transl Neurosci* 2012; 3: 334-344.
- [4] Verkhratsky A, Nedergaard M, Hertz L. Why are astrocytes important? *Neurochem Res* 2015; 40: 389-401.
- [5] Mayorquin LC, Rodriguez A V, Sutachan J-J, et al. Connexin-mediated functional and metabolic coupling between astrocytes and neurons. *Front Mol Neurosci* 2018; 11: 118.
- [6] Fields RD. Oligodendrocytes changing the rules: action potentials in glia and oligodendrocytes controlling action potentials. *Neurosci* 2008; 14: 540-543.
- [7] Roitbak AI, Fanardjian V V. Depolarization of cortical glial cells in response to electrical stimulation of the cortical surface. *Neuroscience* 1981; 6: 2529-2537.
- [8] Agnesi F, Blaha CD, Lin J, et al. Local glutamate release in the rat ventral lateral thalamus evoked by high-frequency stimulation. *J Neural Eng* 2010; 7: 26009.
- [9] Vallejo R, Gupta A, Cedeno DL, et al. Clinical Effectiveness and Mechanism of Action of Spinal Cord Stimulation for Treating Chronic Low Back and Lower Extremity Pain: a Systematic Review. *Curr Pain Headache Rep* 2020; 24: 1-13.
- [10] Mills SEE, Nicolson KP, Smith BH. Chronic pain: a review of its epidemiology and associated factors in population-based studies. *Br J Anaesth* 2019; 123: e273–e283.
- [11] Bennett GJ, Xie Y-K. A peripheral mononeuropathy in rat that produces disorders of pain sensation like those seen in man. *Pain* 1988; 33: 87-107.
- [12] Shu B, He S-Q, Guan Y. Spinal Cord Stimulation Enhances Microglial Activation in the Spinal Cord of Nerve-Injured Rats. *Neurosci Bull* 2020; 36: 1441-1453.
- [13] Wallin J, Cui J-G, Yakhnitsa V, et al. Gabapentin and pregabalin suppress tactile allodynia and potentiate spinal cord stimulation in a model of neuropathy. *Eur J Pain* 2002; 6: 261-272.
- [14] Cui J-G, Sollevi A, Linderroth B, et al. Adenosine receptor activation suppresses tactile hypersensitivity and potentiates spinal cord stimulation in mononeuropathic rats. *Neurosci Lett* 1997; 223: 173-176.
- [15] Yuan B, Liu D, Liu X. Spinal cord stimulation exerts analgesia effects in chronic constriction injury rats via suppression of the TLR4/NF- $\kappa$ B pathway. *Neurosci Lett* 2014; 581: 63-68.
- [16] Xu L, Liu Y, Sun Y, et al. Analgesic effects of TLR4/NF- $\kappa$ B signaling pathway inhibition on chronic neuropathic pain in rats following chronic constriction injury of the sciatic nerve. *Biomed Pharmacother* 2018; 107: 526-533.
- [17] Reddy CG, Miller JW, Abode-Iyamah KO, et al. Ovine model of neuropathic pain for assessing mechanisms of spinal cord stimulation therapy via dorsal horn recordings, von Frey filaments, and gait analysis. *J Pain Res* 2018; 11: 1147-1162.
- [18] Zhang TC, Janik JJ, Peters R V, et al. Spinal sensory projection neuron

responses to spinal cord stimulation are mediated by circuits beyond gate control. *J Neurophysiol* 2015; 114: 284-300.

[19] Seltzer Z, Dubner R, Shir Y. A novel behavioral model of neuropathic pain disorders produced in rats by partial sciatic nerve injury. *Pain* 1990; 43: 205-218.

[20] Meuwissen KP V, de Vries LE, Gu JW, et al. Burst and tonic spinal cord stimulation both activate spinal GABAergic mechanisms to attenuate pain in a rat model of chronic neuropathic pain. *Pain Pract* 2020; 20: 75-87.

[21] Smits H, Van Kleef M, Joosten EA. Spinal cord stimulation of dorsal columns in a rat model of neuropathic pain: evidence for a segmental spinal mechanism of pain relief. *Pain* 2012; 153: 177-183.

[22] Meuwissen KP V, van der Toorn A, Gu JW, et al. Active Recharge Burst and Tonic Spinal Cord Stimulation Engage Different Supraspinal Mechanisms: a Functional Magnetic Resonance Imaging Study in Peripherally Injured Chronic Neuropathic Rats. *Pain Pract* 2020; 20: 510-521.

[23] Truin M, Janssen SPM, van Kleef M, et al. Successful pain relief in non-responders to spinal cord stimulation: the combined use of ketamine and spinal cord stimulation. *Eur J Pain* 2011; 15: 1049-e1-e9.

[24] Meuwissen KP V, Gu JW, Zhang TC, et al. Conventional-SCS vs. burst-SCS and the behavioral effect on mechanical hypersensitivity in a rat model of chronic neuropathic pain: effect of amplitude. *Neuromodulation* 2018; 21: 19-30.

[25] Truin M, van Kleef M, Verboeket Y, et al. The effect of Spinal Cord Stimulation in mice with chronic

neuropathic pain after partial ligation of the sciatic nerve. *Pain* 2009; 145: 312-318.

[26] Meuwissen KP V, van Beek M, Joosten EA. Burst and tonic spinal cord stimulation in the mechanical conflict-avoidance system: Cognitive-motivational aspects. *Neuromodulation* 2020; 23: 605-612.

[27] Yakhnitsa V, Linderroth B, Meyerson BA. Spinal cord stimulation attenuates dorsal horn neuronal hyperexcitability in a rat model of mononeuropathy. *Pain* 1999; 79: 223-233.

[28] Stiller C-O, Cui J-G, O'Connor WT, et al. Release of  $\gamma$ -aminobutyric acid in the dorsal horn and suppression of tactile allodynia by spinal cord stimulation in mononeuropathic rats. *Neurosurgery* 1996; 39: 367-375.

[29] Song Z, Meyerson BA, Linderroth B. Muscarinic receptor activation potentiates the effect of spinal cord stimulation on pain-related behavior in rats with mononeuropathy. *Neurosci Lett* 2008; 436: 7-12.

[30] Simpson RK, Gondo M, Robertson CS, et al. Reduction in the mechanonociceptive response by intrathecal administration of glycine and related compounds. *Neurochem Res* 1996; 21: 1221-1226.

[31] Cui J-G, Meyerson BA, Sollevi A, et al. Effect of spinal cord stimulation on tactile hypersensitivity in mononeuropathic rats is potentiated by simultaneous GABAB and adenosine receptor activation. *Neurosci Lett* 1998; 247: 183-186.

[32] Truin M, van Kleef M, Linderroth B, et al. Increased efficacy of early spinal cord stimulation in an animal model of neuropathic pain. *Eur J Pain* 2011; 15: 111-117.

- [33] Janssen SP, Gerard S, Raijmakers ME, et al. Decreased intracellular GABA levels contribute to spinal cord stimulation-induced analgesia in rats suffering from painful peripheral neuropathy: The role of KCC2 and GABA<sub>A</sub> receptor-mediated inhibition. *Neurochem Int* 2012; 60: 21-30.
- [34] Truin M, Van Venrooij P, Duysens V, et al. Spinal cord stimulation in a mouse chronic neuropathic pain model. *Neuromodulation* 2007; 10: 358-362.
- [35] Li D, Yang H, Meyerson BA, et al. Response to spinal cord stimulation in variants of the spared nerve injury pain model. *Neurosci Lett* 2006; 400: 115-120.
- [36] Schechtmann G, Song Z, Ultenius C, et al. Cholinergic mechanisms involved in the pain relieving effect of spinal cord stimulation in a model of neuropathy. *Pain* 2008; 139: 136-145.
- [37] Sun L, Tai L, Qiu Q, et al. Endocannabinoid activation of CB1 receptors contributes to long-lasting reversal of neuropathic pain by repetitive spinal cord stimulation. *Eur J Pain* 2017; 21: 804-814.
- [38] Meuwissen KP V, Gu JW, Zhang TC, et al. Burst spinal cord stimulation in peripherally injured chronic neuropathic rats: a delayed effect. *Pain Pract* 2018; 18: 988-996.
- [39] Song Z, Meyerson BA, Linderoth B. Spinal 5-HT receptors that contribute to the pain-relieving effects of spinal cord stimulation in a rat model of neuropathy. *Pain* 2011; 152: 1666-1673.
- [40] Smits H, Kleef M V, Honig W, et al. Spinal cord stimulation induces c-Fos expression in the dorsal horn in rats with neuropathic pain after partial sciatic nerve injury. *Neurosci Lett* 2009; 450: 70-73.
- [41] Decosterd I, Woolf CJ. Spared nerve injury: An animal model of persistent peripheral neuropathic pain. *Pain* 2000; 87: 149-158.
- [42] Tilley DM, Vallejo R, Kelley CA, et al. A continuous spinal cord stimulation model attenuates pain-related behavior in vivo following induction of a peripheral nerve injury. *Neuromodulation* 2015; 18: 171-176.
- [43] Vallejo R, Gupta A, Kelley CA, et al. Effects of Phase Polarity and Charge Balance Spinal Cord Stimulation on Behavior and Gene Expression in a Rat Model of Neuropathic Pain. *Neuromodulation* 2020; 23: 26-35.
- [44] Vallejo R, Tilley DM, Cedeño DL, et al. Genomics of the Effect of Spinal Cord Stimulation on an Animal Model of Neuropathic Pain. *Neuromodulation* 2016; 19: 576-586.
- [45] Smits H, Ultenius C, Deumens R, et al. Effect of spinal cord stimulation in an animal model of neuropathic pain relates to degree of tactile “allodynia”. *Neuroscience* 2006; 143: 541-546.
- [46] Sato KL, Sanada LS, Da Silva MD, et al. Transcutaneous electrical nerve stimulation, acupuncture, and spinal cord stimulation on neuropathic, inflammatory and, non-inflammatory pain in rat models. *Korean J Pain* 2020; 33: 121.
- [47] Sato KL, King EW, Johanek LM, et al. Spinal cord stimulation reduces hypersensitivity through activation of opioid receptors in a frequency-dependent manner. *Eur J Pain* 2013; 17: 551-561.
- [48] Sato KL, Johanek LM, Sanada LS, et al. Spinal cord stimulation reduces mechanical hyperalgesia and glial cell activation in animals with neuropathic pain. *Anesth Analg* 2014; 118: 464-472.

- [49] Song Z, Viisanen H, Meyerson BA, et al. Efficacy of kilohertz-frequency and conventional spinal cord stimulation in rat models of different pain conditions. *Neuromodulation* 2014; 17: 226-235.
- [50] Vallejo R, Kelley CA, Gupta A, et al. Modulation of neuroglial interactions using differential target multiplexed spinal cord stimulation in an animal model of neuropathic pain. *Mol Pain* 2020; 16: 1744806920918057.
- [51] Cedeño DL, Smith WJ, Kelley CA, et al. Spinal cord stimulation using differential target multiplexed programming modulates neural cell-specific transcriptomes in an animal model of neuropathic pain. *Mol Pain* 2020; 16: 1744806920964360.
- [52] Ho Kim S, Mo Chung J. An experimental model for peripheral neuropathy produced by segmental spinal nerve ligation in the rat. *Pain* 1992; 50: 355-363.
- [53] Shechter R, Yang F, Xu Q, et al. Conventional and kilohertz-frequency spinal cord stimulation produces intensity- and frequency-dependent inhibition of mechanical hypersensitivity in a rat model of neuropathic pain. *Anesthesiol* 2013; 119: 422-432.
- [54] Chen Z, Huang Q, Yang F, et al. The impact of electrical charge delivery on inhibition of mechanical hypersensitivity in nerve-injured rats by sub-sensory threshold spinal cord stimulation. *Neuromodulation* 2019; 22: 163-171.
- [55] Sivanesan E, Stephens KE, Huang Q, et al. Spinal cord stimulation prevents paclitaxel-induced mechanical and cold hypersensitivity and modulates spinal gene expression in rats. *Pain Reports* 2019; 4: e7854.
- [56] Hopkins HL, Duggett NA, Flatters SJL. Chemotherapy-induced painful neuropathy: pain-like behaviours in rodent models and their response to commonly-used analgesics. *Curr Opin Support Palliat Care* 2016; 10: 119-128.
- [57] Stephens KE, Chen Z, Sivanesan E, et al. RNA-seq of spinal cord from nerve-injured rats after spinal cord stimulation. *Mol Pain* 2018; 14: 1744806918817429.
- [58] Furman BL. Streptozotocin-induced diabetic models in mice and rats. *Curr Protoc Pharmacol* 2015; 70: 5-47.
- [59] Wu M, Thorkilsen MM, Qin C, et al. Effects of spinal cord stimulation on peripheral blood circulation in rats with streptozotocin-induced diabetes. *Neuromodulation* 2007; 10: 216-223.
- [60] Van Beek M, Van Kleef M, Linderoth B, et al. Spinal cord stimulation in experimental chronic painful diabetic polyneuropathy: delayed effect of high-frequency stimulation. *Eur J Pain* 2017; 21: 795-803.
- [61] van Beek M, Hermes D, Honig WM, et al. Long-term spinal cord stimulation alleviates mechanical hypersensitivity and increases peripheral cutaneous blood perfusion in experimental painful diabetic polyneuropathy. *Neuromodulation* 2018; 21: 472-479.
- [62] Ren K, Dubner R. Inflammatory models of pain and hyperalgesia. *ILAR J* 1999; 40: 111-118.
- [63] Cui J-G, Meyerson BA, Linderoth B. Opposite effects of spinal cord stimulation in different phases of carrageenan-induced hyperalgesia. *Eur J Pain* 1999; 3: 365-374.
- [64] Woolf CJ, Doubell TP. The pathophysiology of chronic pain—increased sensitivity to low threshold A $\beta$ -fibre inputs. *Curr Opin Neurobiol* 1994; 4: 525-534.

- [65] Lindblom U, Meyerson BA. Influence on touch, vibration and cutaneous pain of dorsal column stimulation in man. *Pain* 1975; 1: 257-270.
- [66] Lindblom U, Meyerson BA. On the effect of electrical stimulation of the dorsal column system on sensory thresholds in patients with chronic pain. In: *Progress in brain research*. Elsevier, 1976, pp. 237-241.
- [67] Linderoth B, Meyerson BA. Spinal Cord Stimulation Exploration of the Physiological Basis of a Widely Used Therapy. *Anesthesiol* 2010; 113: 1265-1267.
- [68] Radhakrishnan R, Moore SA, Sluka KA. Unilateral carrageenan injection into muscle or joint induces chronic bilateral hyperalgesia in rats. *Pain* 2003; 104: 567-577.
- [69] Sato KL, Johanek LM, Sanada LS, et al. Spinal cord stimulation (scs) improves decreased physical activity induced by nerve injury. *Behav Neurosci* 2014; 128: 625-632.
- [70] Foreman RD, Linderoth B. Neural mechanisms of spinal cord stimulation. In: *International review of neurobiology*. Elsevier, 2012, pp. 87-119.
- [71] Linderoth B, Gunasekera L, Meyerson BA. Effects of sympathectomy on skin and muscle microcirculation during dorsal column stimulation: animal studies. *Neurosurgery* 1991; 29: 874-879.
- [72] Croom JE, Foreman RD, Chandler MJ, et al. Reevaluation of the role of the sympathetic nervous system in cutaneous vasodilation during dorsal spinal cord stimulation: are multiple mechanisms active? *Neuromodulation* 1998; 1: 91-101.
- [73] Wu M, Linderoth B, Foreman RD. Putative mechanisms behind effects of spinal cord stimulation on vascular diseases: a review of experimental studies. *Auton Neurosci* 2008; 138: 9-23.
- [74] Vallejo R, Vera-Portocarrero L, Kelley C, et al. Translational comparison of rodent and sheep models of continuous differential target multiplexed spinal cord stimulation. In: *14th International Neuromodulation Society Congress*. Sydney, Australia, 2019.
- [75] Wilkes D, Li G, Angeles CF, et al. A large animal neuropathic pain model in sheep: a strategy for improving the predictability of preclinical models for therapeutic development. *J Pain Res* 2012; 5: 415-424.